(107) Obituary, *MNRAS*, **74**, 275, 1915.
(108) A. D. Andrews, *Irish AJ*, **20**, 102, 1992.
(109) J. Foster, *Alumni Oxonienses, 1715–1886*, vol. 3, p. 842, 1891.
(110) https://amounderness.co.uk/seafield_house_article.html
(111) Obituary, *MNRAS*, **72**, 246, 1912.
(112) E. T. Whittaker, *MNRAS*, **62**, 186, 1902.
(113) Obituary Notices, *MNRAS*, **117**, 256, 1957.
(114) Obituaries, *Journal of the Iron and Steel Institute, Proceedings*, vol. 81, part 1, p. 513, 1910.
(115) W. Orchiston, *BAA Historical Section Newsletter*, **25**, 12, 2022.
(116) Obituaries, *Proceedings of the Institution of Civil Engineers*, vol. 201, part 1, p. 403, 1916.
(117) A. R. Clapham, *Biographical Memoirs of Fellows of the Royal Society*, vol. 17, issue 17, p. 511, 1971.
(118) The Department of Education at the University of Manchester, 1890–1911, *University of Manchester Publications* No. 58, p. 114, 1911.
(119) Fellows Elected, *MNRAS*, **61**, 165, 1901.
(120) Obituary, *MNRAS*, **99**, 297, 1939.
(121) The Transit of Venus 1874, *MNRAS*, **35**, 1875.

REDISCUSSION OF ECLIPSING BINARIES. PAPER 18: THE A-TYPE SYSTEM OO PEGASI

By John Southworth

Astrophysics Group, Keele University

OO Peg is a detached eclipsing binary system containing two late-A-type stars in a circular orbit with a period of 2·985 d. Using published spectroscopic results and a light-curve from the *Transiting Exoplanet Survey Satellite* (*TESS*) we determine their masses to be 1·69 ± 0·09 and 1·74 ± 0·06 $M_{\odot}$ and their radii to be 2·12 ± 0·03 and 1·91 ± 0·03 $R_{\odot}$. The *TESS* data are of high quality, but discrepancies in the radial velocities from two sources prevent a precise mass measurement. The primary star is definitively hotter, larger, and more luminous than its companion, but its mass is lower (albeit to a significance of only 1·1σ). Using published apparent magnitudes and temperatures, we find a distance of 238·8 ± 6·1 pc, in agreement with the *Gaia* DR3 parallax. Although both components are in the δ Scuti instability strip, we find no evidence of pulsations. More extensive spectroscopy is needed to improve our understanding of the system.

Introduction

In this series of papers[1] we have been systematically reanalysing known detached eclipsing binaries (dEBs) in order to determine their physical properties to high precision. The main improvements *versus* previous work stem from the availability of high-quality light-curves from space missions such as *Kepler*[2] and *TESS* (*Transiting Exoplanet Survey Satellite*[3]) — see ref. 4 for a review.

This work is important because dEBs are our primary source of direct measurements of the basic properties (mass and radius) of normal stars[5,6]. They are widely used to calibrate physical processes included in theoretical models of stellar evolution[7,8], such as atomic diffusion[9], convective-core overshooting[10], and the size of the core[11]. A high precision in the measurements of the stellar properties is vital for reliable results[12] and can approach 0·2% precision in mass and radius in the best cases[13].

OO Pegasi

In this work we present an analysis of OO Pegasi (Table I) based on published spectroscopy and new space-based photometry. The eclipsing nature of OO Peg was found using data from the *Hipparcos* satellite[16,22]. A first detailed analysis was presented by Munari *et al.*[23] (hereafter M01) with the aim of assessing the expected quality of results from the then-forthcoming *Gaia* mission; of the three systems in that paper V505 Per and V570 Per have already been revisited by the present author using the new *TESS* data[24,25]. M01 used only *Hipparcos* photometry and radial-velocity (RV) measurements from ground-based spectroscopy in the 850–875-nm region, to represent the type of observations that *Gaia* was expected to obtain. Due to these limitations they were only able to obtain masses to 2% and radii to 4% precision.

A subsequent analysis of OO Peg was presented by Çakırlı[21] (hereafter C15) who added new spectroscopic RV measurements and a more extensive light-curve from the All Sky Automated Survey (ASAS[26]) to determine the properties of the components more precisely. C15 also measured the atmospheric parameters of the components, their projected rotational velocities, and the reddening and distance of the system. He searched for but found no evidence of pulsations in the light-curves from *Hipparcos* and ASAS, despite both components being in the δ Scuti instability strip[27].

TABLE I

Basic information on OO Pegasi.

Property	*Value*	*Reference*
Right ascension (J2000)	$21^h41^m37^s\!.70$	14
Declination (J2000)	$+14°39'30''\!.8$	14
Henry Draper designation	HD 206417	15
Hipparcos designation	HIP 107099	16
Gaia DR3 designation	1770729907069675392	14
Gaia DR3 parallax	4·2534 ± 0·0245 mas	14
TESS Input Catalog designation	TIC 314847177	17
U magnitude	8·650 ± 0·010	18
B magnitude	8·635 ± 0·021	19
V magnitude	8·354 ± 0·018	19
J magnitude	7·676 ± 0·023	20
H magnitude	7·633 ± 0·027	20
K_s magnitude	7·555 ± 0·018	20
Spectral type	A7 V + A8 V	21

The apparent mangitudes in Table I come from a variety of sources. The U magnitude is from Oja[18] and relies on just two observations so may not reflect the brightness of the system outside eclipse. This number is not used in our analysis, but the consistency between the distances measured in the various passbands (see below) suggests it does represent an out-of-eclipse measurement. The BV magnitudes are from the *Tycho* experiment[19] on the *Hipparcos* satellite and each comprise the average of 55 measurements well-distributed in orbital phase. The JHK_s magnitudes are from 2MASS[20] and were obtained at a single epoch corresponding to orbital phase 0·615, which is not within an eclipse.

Photometric observations

OO Peg has been observed just once by *TESS*, in sector 55, beginning on 2022/08/05 and concluding on 2022/09/01. A second set of observations is scheduled for sector 82 and will occur in 2024 August if the spacecraft remains healthy. The observations from sector 55 were obtained with a cadence of 600 s, which is lower than desired and decreases the information content of the data.

The available light-curve from *TESS* was downloaded from the NASA Mikulski Archive for Space Telescopes (MAST*) using the LIGHTKURVE package[28]. We used the simple aperture photometry (SAP) data from the *TESS*–SPOC data reduction[29]. A quality flag of "hard" yielded a total of 3412 data points (Fig. 1). We rejected the data in the time interval BJD_{TDB} 2459804·25 to 2459811·70 to avoid a stretch of data with the eclipses either partially covered or not observed at all, leaving 2831 data points for further analysis. These were normalized using LIGHTKURVE, converted to differential magnitude, and the median magnitude of the sector subtracted.

A query of the *Gaia* DR3 database† returned a total of 56 objects within 2 arcmin of OO Peg. Of these, the brightest is fainter by 4·23 mag in the G band and 3·98 mag in the G_{RP} band. A small amount of third light is therefore expected to contaminate the *TESS* light-curve of OO Peg, at the level of approximately 1%.

Light-curve analysis

The components of OO Peg are small compared to their orbital separation, so the system is suitable for analysis with the JKTEBOP‡ code[30,31], for which we used version 43. We defined the primary eclipse to be the deeper of the two eclipses, star A to be the component eclipsed at primary eclipse, star B to be its companion, and the primary eclipse to occur at orbital phase zero. In the case of OO Peg star A is both hotter and larger than star B, by small but significant amounts.

The JKTEBOP fitted parameters included the fractional radii of the stars (r_A and r_B), expressed as their sum ($r_A + r_B$) and ratio ($k = r_B/r_A$), the central surface-brightness ratio (J), orbital inclination (i), orbital period (P), and a reference time of primary minimum (T_0). A circular orbit was assumed, after confirming that allowing for orbital eccentricity has a negligible effect on the values of the fitted parameters.

* https://mast.stsci.edu/portal/Mashup/Clients/Mast/Portal.html

† https://vizier.cds.unistra.fr/viz-bin/VizieR-3?-source=I/355/gaiadr3

‡ http://www.astro.keele.ac.uk/jkt/codes/jktebop.html

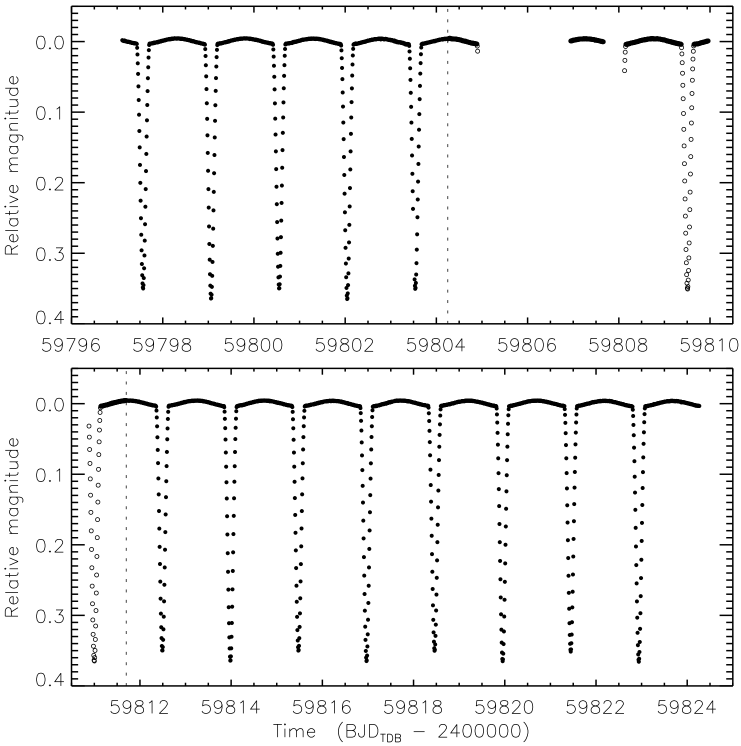

FIG. 1

TESS short-cadence SAP photometry of OO Peg. The flux measurements have been converted to magnitude units then rectified to zero magnitude by subtraction of the median. The data rejected from the analysis are shown using open circles, and the corresponding cutoff times indicated with vertical dashed lines.

Initial attempts to fit for third light returned values that were very small and slightly less than zero. An experiment with it fixed to a value of 2%, to account for the nearby stars discussed above, yielded a solution with significantly larger residuals and a noticably poorer fit to the eclipses. We therefore fixed third light to zero.

Limb darkening was included using the power-2 law[32–34] defined according to

$$\frac{F(\mu)}{F(1)} = 1 - c(1 - \mu^{\alpha}), \tag{1}$$

where $\mu = \cos\gamma$, γ is the angle between the observer's line of sight and the surface normal, $F(\mu)$ is the surface brightness at position μ on the stellar disc, c is the linear coefficient, and α is the nonlinear coefficient. As the two stars are very similar we assumed their limb-darkening behaviours to be identical. Initial fits showed that we were able to fit for one but not both of the limb-darkening coefficients, so we fitted for c and left α fixed at a theoretical value[35,36].

The relatively low 600-s sampling rate of the *TESS* data was accounted for by numerically integrating the model to match[37]. In effect we calculated the model at five points, each spaced by 120 s, and averaged the results before comparing to an observed data point. We found that this had a negligible effect on the results, but continued to do so as the increase in computation time was not a problem. The coefficients of two quadratic functions, one for each half of the *TESS* sector, were also included to normalize precisely the light-curve to zero differential magnitude.

We found no evidence for changes in the orbital period for OO Peg, in agreement with the results of C15. We therefore included the observed time of primary minimum from the *Hipparcos* light-curve calculated by M01 (2448499·1545 ± 0·0020) to help constrain the orbital ephemeris more precisely. This step lowered the uncertainty in P by approximately a factor of three.

The resulting best fit is shown in Fig. 2 and the parameters are given in Table II. Uncertainties in the fitted parameters were calculated using both Monte Carlo and residual-permutation simulations[38,39], and the larger of the two options chosen for each parameter. The two error-estimation algorithms were in good agreement for all parameters, as expected because there is no obvious systematic noise present in the data. The uncertainties in the all-important fractional radii are encouragingly low at 0·17% and 0·27%, despite the relatively poor sampling rate of the *TESS* photometry.

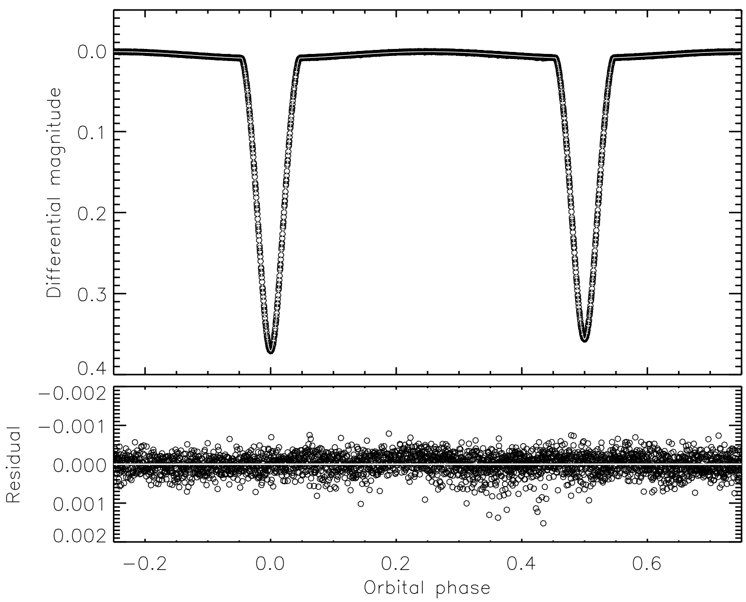

Fig. 2

The 600-s cadence *TESS* light-curves of OO Peg (open circles) and its best fit from JKTEBOP (white-on-black line) *versus* orbital phase. The residuals are shown on an enlarged scale in the lower panel.

TABLE II

Parameters of OO Peg, with their 1σ uncertainties, measured from the TESS sector-55 light-curves using the JKTEBOP code.

Parameter	*Value*
Fitted parameters:	
Primary eclipse time (BJD_{TDB})	2459813·984151 ± 0·000007
Orbital period (d)	2·98465593 ± 0·00000049
Orbital inclination (°)	83·629 ± 0·013
Sum of the fractional radii	0·30576 ± 0·00020
Ratio of the radii	0·8983 ± 0·0038
Central-surface-brightness ratio	0·96661 ± 0·00016
LD coefficient c	0·709 ± 0·014
LD coefficient α	0·431 (fixed)
Derived parameters:	
Fractional radius of star A	0·16107 ± 0·00028
Fractional radius of star B	0·14489 ± 0·00039
Light ratio ℓ_B/ℓ_A	0·7794 ± 0·0065

Radial-velocity analysis

M01 published a set of 21 RVs for each component of OO Peg, which are tabulated in the paper. The spectra on which they were based were deliberately obtained at quasi-random times in order to simulate a dataset that might be expected from *Gaia*. As a result, two spectra are too blended to give precise RVs and there is only one spectrum near second quadrature. We reanalysed the RVs from M01 to confirm their results, and followed those authors in omitting the RVs from the two most blended spectra.

To fit the RVs we used JKTEBOP and the orbital ephemeris from Table II. The fitted parameters were the velocity amplitudes of the two stars, K_A and K_B, and the systemic velocity (V_γ) of the two stars. We also allowed for a change in T_0 to insure against ephemeris drift or period changes, but all solutions were consistent with the ephemeris given in Table II. Separate fits were obtained with V_γ either assumed to be the same for the two stars or allowed to be different. The error bars of the RVs for each star were scaled to give a reduced χ^2 of $\chi^2_\nu = 1{\cdot}0$ *versus* the best fit. Parameter uncertainties were calculated using the Monte Carlo procedure[24]. The results are given in Table III.

It was immediately clear that our star A is the *secondary* component for M01, something that can happen easily when the primary and secondary eclipses are of similar depth and the photometric data are quite scattered. We accounted for this in our analysis. We note that this is also apparent in C15 (see his fig. 4) but not commented on by that author. Our K_A agrees with M01, but our K_B and V_γ do not agree within the uncertainties. We also notice that there is a counterintuitive result that the r.m.s. residuals are lower for star A when the V_γ values of the two stars are required to be the same — this occurs because of the rescaling of the RV uncertainties combined with the RV measurements having a range of uncertainties.

C15 obtained 15 spectra of OO Peg from which 15 RVs were obtained for star A and 14 for star B. C15 fitted spectroscopic orbits to the spectra from his own observations together with those from M01. We first modelled the RVs from C15 separately. Four of the RVs for star A and three for star B are close to conjunction so suffer from blending and contribute little to pinning down

K_A and K_B, so we ran solutions with those omitted. The results were similar to those for all RVs, and we adopted them as our standard datasets for the RVs from C15.

Table III shows that there are significant discrepancies between the solutions of different RV datasets, both calculated in this work and *versus* the literature. We also consistently find that K_A is larger than K_B, thus star A is less massive than star B (although the difference is of similar size to the uncertainties). Some of these discrepancies are driven by small-number statistics, and some are likely due to differences in V_γ from the differing RV-measurement processes used by M01 and C15. The biggest discrepancy is in the K_B values from the two sources of RVs, which differ by 4 km s^{-1}.

We made the choice to fit the RVs from M01 and C15 simultaneously, both with the combined and independent V_γ values (Fig. 3). In each case we scaled the error bars of the individual datasets to give $\chi^2_\nu = 1$ and subtracted the best-fitting V_γ before fitting the combined data. Our results are in between those for the two RV sources separately, as expected. The K_A values are consistent over all solutions so we adopt a value of $112{\cdot}6 \pm 1{\cdot}2$ km s^{-1}. The error bar is the quadrature addition of the 1·1 km s^{-1} uncertainty in Table III and the 0·5 km s^{-1} which is the largest difference between the adopted K_A and the other fitted values.

For K_B we adopt a value of $109{\cdot}1 \pm 2{\cdot}8$ km s^{-1}, where the uncertainty is the quadrature addition of 0·9 km s^{-1} and 2·7 km s^{-1} following the same argument. This K_B is unfortunately rather uncertain, which prevents the measurement of the masses of the stars to high precision.

Physical properties and distance to OO Peg

Using the photometric and spectroscopic results from Tables I, II, and III, we have determined the physical properties of the OO Peg system using the JKTABSDIM code[41]. The results are given in Table IV and show that the masses are measured to 5·2% (star A) and 3·3% (star B), and the radii to 1·4% (both stars). This is not the desired 2% precision[5,42] due to the uncertainty in the value of K_B. The mass measurements agree well with those of M01 but not C15; the radius measurements disagree with both. In particular, the R_B value from M01 ($1{\cdot}37 \pm 0{\cdot}05\ R_\odot$) is extremely low. Our results are based on a careful analysis of

TABLE III

Spectroscopic orbits for OO Peg from the literature and from the reanalysis of the RVs in the current work. K_A and K_B values values were not given by M01, so we have calculated the values that would reproduce their mass measurements. All quantities are in km s^{-1}.

Source	K_A	K_B	$V\gamma$	$V\gamma_{,A}$	$V\gamma_{,B}$	*r.m.s residual star A*	*star B*
M01 (our calculation)	112·0	110·1	8·47±0·46				
C15	111±2	114±3	6·7±0·1				
M01 (our calculation)	112·1±1·6	107·6±1·0	10·8±0·7			5·1	6·7
M01 (our calculation)	112·4±1·7	107·6±1·0		11·4±1·2	10·5±0·8	5·4	6·6
C15 (our fit, V_γ same)	112·9±1·6	111·8±1·2	5·5±0·9			5·1	3·2
C15 (our fit, V_γ different)	112·3±1·5	111·5±1·3		7·6±1·2	3·9±1·2	4·2	3·1
Combined (V_γ same)	112·7±1·1	109·1±0·9	0·2±0·7			5·1	5·9
Combined (V_γ different)	112·5±1·0	109·0±0·9		0·3±0·8	−0·4±0·7	5·1	5·6
Adopted values	112·6±1·2	109·1±2·8					

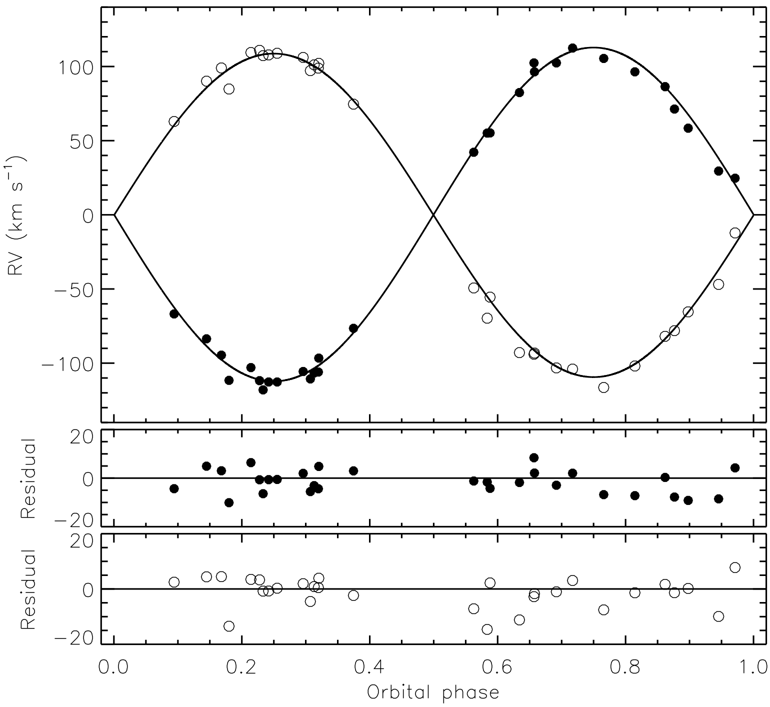

FIG. 3

RVs of OO Peg from M01 and C15 (filled circles for star A and open circles for star B), compared to the best fit from JKTEBOP (solid lines) with a separate V_γ value for each star. The residuals are given in the lower panels separately for the two components.

TABLE IV

Physical properties of OO Peg defined using the nominal solar units given by IAU 2015 Resolution B3 (ref. 40). The $T_{\rm eff}$ values are from C15.

Parameter	*Star A*	*Star B*
Mass ratio $M_{\rm B}/M_{\rm A}$	1·032 ± 0·029	
Semi-major axis of relative orbit ($\mathcal{R}^{\rm N}_\odot$)	13·16 ± 0·18	
Mass ($\mathcal{M}^{\rm N}_\odot$)	1·689 ± 0·088	1·744 ± 0·058
Radius ($\mathcal{R}^{\rm N}_\odot$)	2·120 ± 0·029	1·907 ± 0·027
Surface gravity (log[cgs])	4·013 ± 0·011	4·119 ± 0·005
Density ($\rho_\odot$)	0·1774 ± 0·0027	0·2515 ± 0·0040
Synchronous rotational velocity (km s^{-1})	35·93 ± 0·50	32·32 ± 0·45
Effective temperature (K)	7850 ± 350	7600 ± 450
Luminosity log($L/\mathcal{L}^{\rm N}_\odot$)	1·19 ± 0·08	1·04 ± 0·10
$M_{\rm bol}$ (mag)	1·77 ± 0·20	2·14 ± 0·26
Interstellar reddening $E(B-V)$ (mag)	0·09 ± 0·02	
Distance (pc)	238·8 ± 6·1	

the available RVs and much higher-quality light-curves from *TESS*, so should be preferred to previous values.

M01 determined the effective temperatures ($T_{\rm eff}$s) of the stars from a comparison between the observed and synthetic spectra, finding $T_{\rm eff,A} = 8770 \pm 150$ K and $T_{\rm eff,B} = 8683 \pm 180$ K. The ratio of these values agrees well with the surface-brightness ratio measured from the light-curve (Table II). Using these $T_{\rm eff}$s and the apparent magnitudes of the system (Table I), we determined the distance to OO Peg using the *K*-band surface-brightness method[41] and calibrations from Kervella *et al.*[43]. The interstellar reddening was determined by requiring the *UBV* and *JHK* distances to agree, *via* manual iteration, resulting in $E(B-V) = 0{\cdot}21 \pm 0{\cdot}03$ mag and a distance of $245{\cdot}2 \pm 4{\cdot}9$ pc. This reddening is rather larger than expected — the STILISM* on-line tool[44,45] gives a value of $0{\cdot}037 \pm 0{\cdot}018$ mag — and the distance is also 2σ beyond the value *Gaia* DR3[14] value of $234{\cdot}1 \pm 1{\cdot}3$ pc.

C15 determined rather smaller temperatures of $T_{\rm eff,A} = 7850 \pm 350$ K and $T_{\rm eff,B} = 7600 \pm 450$ K, *via* comparison with reference-star spectra. Using these values instead of the ones from M01, we obtain $E(B-V) = 0{\cdot}09 \pm 0{\cdot}02$ mag and a distance of $238{\cdot}8 \pm 6{\cdot}1$ pc. This $E(B-V)$ is in much better agreement with the STILISM value, and the distance is also consistent with the *Gaia* DR3 parallax at the $0{\cdot}8\sigma$ level. We therefore adopt these $T_{\rm eff}$s and $E(B-V)$ as our final values in Table IV. Supporting evidence for these lower temperatures are the catalogue $T_{\rm eff}$s of 7476 ± 149 K given in v8 of the *TESS* Input Catalog[17] and 7347 ± 17 K from the *Gaia* DR3 APSIS pipeline[46,47]. Both catalogues treat point sources as single stars, but in the case of OO Peg this is a reasonable approximation due to the similarity of the two components.

C15 measured $E(B-V) = 0{\cdot}29 \pm 0{\cdot}01$ from the strength of the interstellar Na *D* lines; such a large reddening is highly inconsistent with our results and would require the stars to have $T_{\rm eff}$s in the region of 10 000 K for the distances measured in the optical to match those measured in the IR.

Summary and final points

OO Peg is a dEB containing two components with late-A spectral types, on a circular orbit with a period of 2·98 d, whose eclipsing nature was discovered thanks to the *Hipparcos* satellite. We have presented a reanalysis of the system based on a space-based light-curve from the *TESS* mission and published spectroscopic parameters. The *TESS* light-curve is of high quality and allows the fractional radii of the stars to be determined to 0·2% precision; star A is clearly larger, hotter, and more luminous than its companion. However, our reanalysis of published RVs from two sources yields both a disagreement in the value of $K_{\rm B}$ and the measurement of a lower mass for star A than star B. This discrepancy would be problematic for stellar evolutionary theory, but is thankfully not significant due to the uncertainty in the measured masses. Using published apparent magnitudes of the system and $T_{\rm eff}$ values of the stars, we have determined a distance to the system in agreement with the *Gaia* DR3 parallax.

Both components of OO Peg are in a region of the luminosity *versus* $T_{\rm eff}$ diagram where a high fraction of stars show δ Scuti pulsations[27], but are not known to pulsate. We therefore calculated a Fourier transform of the residuals of the JKTEBOP fit using version 1.2.0 of the PERIOD04 code[48]. No significant periodicity was found up to the Nyquist frequency of 72 d^{-1}, with a noise level

*https://stilism.obspm.fr

of approximately 0·01 mmag from 1 d^{-1} to the Nyquist frequency. Lower-amplitude pulsations may be present but would require significantly more photometry to measure.

We made a brief comparison of the masses, radii, and $T_{\rm eff}$s of the stars to the PARSEC 1·2S theoretical stellar-evolutionary models[49,50]. Agreement was found for a solar chemical composition and an age of $1{\cdot}0 \pm 0{\cdot}3$ Gyr, which supports the lower $T_{\rm eff}$ values found by C15 *versus* those obtained by M01.

The quality of our results has been limited by the imprecision of the spectroscopic parameters measured for the system: both the RVs and the $T_{\rm eff}$s are quite uncertain. Conversely, the *TESS* data allow high-quality measurements of its photometric parameters. Further work should therefore concentrate on performing a more extensive spectroscopic analysis of OO Peg. Forthcoming data releases from the *Gaia* satellite may well help.

Acknowledgements

We thank the anonymous referee for a helpful report. This paper includes data collected by the *TESS* mission and obtained from the MAST data archive at the Space Telescope Science Institute (STScI). Funding for the *TESS* mission is provided by the NASA's Science Mission Directorate. STScI is operated by the Association of Universities for Research in Astronomy, Inc., under NASA contract NAS 5–26555. This work has made use of data from the European Space Agency (ESA) mission *Gaia**, processed by the *Gaia* Data Processing and Analysis Consortium (DPAC†). Funding for the DPAC has been provided by national institutions, in particular the institutions participating in the *Gaia* Multilateral Agreement. The following resources were used in the course of this work: the NASA Astrophysics Data System; the *Simbad* database operated at CDS, Strasbourg, France; and the arχiv scientific paper preprint service operated by Cornell University.

References

(1) J. Southworth, *The Observatory*, **140**, 247, 2020.
(2) W. J. Borucki, *Reports on Progress in Physics*, **79**, 036901, 2016.
(3) G. R. Ricker *et al.*, *Journal of Astronomical Telescopes, Instruments, and Systems*, **1**, 014003, 2015.
(4) J. Southworth, *Universe*, **7**, 369, 2021.
(5) J. Andersen, *A&ARv*, **3**, 91, 1991.
(6) G. Torres, J. Andersen & A. Giménez, *A&ARv*, **18**, 67, 2010.
(7) E. Lastennet & D. Valls-Gabaud, *A&A*, **396**, 551, 2002.
(8) C. del Burgo & C. Allende Prieto, *MNRAS*, **479**, 1953, 2018.
(9) J. Higl & A. Weiss, *A&A*, **608**, A62, 2017.
(10) A. Claret & G. Torres, *ApJ*, **859**, 100, 2018.
(11) A. Tkachenko *et al.*, *A&A*, **637**, A60, 2020.
(12) G. Valle *et al.*, *A&A*, **615**, A62, 2018.
(13) P. F. L. Maxted *et al.*, *MNRAS*, **498**, 332, 2020.
(14) Gaia Collaboration, *A&A*, **649**, A1, 2021.
(15) A. J. Cannon & E. C. Pickering, *Annals of Harvard College Observatory*, **99**, 1, 1924.
(16) ESA (ed.), *The Hipparcos and Tycho catalogues. ESA Special Publication*, vol. 1200, 1997.
(17) K. G. Stassun *et al.*, *AJ*, **158**, 138, 2019.
(18) T. Oja, *A&AS*, **71**, 561, 1987.
(19) E. Høg *et al.*, *A&A*, **355**, L27, 2000.
(20) R. M. Cutri *et al.*, *2MASS All Sky Catalogue of Point Sources*, NASA/IPAC Infrared Science Archive, Caltech, US), 2003.
(21) Ö. Çakırlı, *New Astronomy*, **37**, 70, 2015.

*https://www.cosmos.esa.int/gaia

†https://www.cosmos.esa.int/web/gaia/dpac/consortium

(22) E. V. Kazarovets *et al.*, *IBVS*, **4659**, 1, 1999.
(23) U. Munari *et al.*, *A&A*, **378**, 477, 2001.
(24) J. Southworth, *The Observatory*, **141**, 234, 2021.
(25) J. Southworth, *The Observatory*, **143**, 165, 2023.
(26) G. Pojmański, *AcA*, **47**, 467, 1997.
(27) S. J. Murphy *et al.*, *MNRAS*, **485**, 2380, 2019.
(28) Lightkurve Collaboration, '(Lightkurve: *Kepler* and *TESS* time series analysis in Python)', Astrophysics Source Code Library, 2018.
(29) J. M. Jenkins *et al.*, in *Proc. SPIE*, 2016, *Society of Photo-Optical Instrumentation Engineers (SPIE) Conference Series*, vol. 9913, p. 99133E.
(30) J. Southworth, P. F. L. Maxted & B. Smalley, *MNRAS*, **351**, 1277, 2004.
(31) J. Southworth, *A&A*, **557**, A119, 2013.
(32) D. Hestroffer, *A&A*, **327**, 199, 1997.
(33) P. F. L. Maxted, *A&A*, **616**, A39, 2018.
(34) J. Southworth, *The Observatory*, **143**, 71, 2023.
(35) A. Claret & J. Southworth, *A&A*, **664**, A128, 2022.
(36) A. Claret & J. Southworth, *A&A*, **674**, A63, 2023.
(37) J. Southworth, *MNRAS*, **417**, 2166, 2011.
(38) J. Southworth, P. F. L. Maxted & B. Smalley, *MNRAS*, **349**, 547, 2004.
(39) J. Southworth, *MNRAS*, **386**, 1644, 2008.
(40) A. Prša *et al.*, *AJ*, **152**, 41, 2016.
(41) J. Southworth, P. F. L. Maxted & B. Smalley, *A&A*, **429**, 645, 2005.
(42) J. Southworth, in *Living Together: Planets, Host Stars and Binaries* (S. M. Rucinski, G. Torres & M. Zejda, eds.), 2015, *Astronomical Society of the Pacific Conference Series*, vol. 496, p. 321.
(43) P. Kervella *et al.*, *A&A*, **426**, 297, 2004.
(44) R. Lallement *et al.*, *A&A*, **561**, A91, 2014.
(45) R. Lallement *et al.*, *A&A*, **616**, A132, 2018.
(46) O. L. Creevey *et al.*, *A&A*, **674**, A26, 2023.
(47) M. Fouesneau *et al.*, *A&A*, **674**, A28, 2023.
(48) P. Lenz & M. Breger, *Communications in Asteroseismology*, **146**, 53, 2005.
(49) A. Bressan *et al.*, *MNRAS*, **427**, 127, 2012.
(50) Y. Chen *et al.*, *MNRAS*, **444**, 2525, 2014.

CORRESPONDENCE

'To the Editors of 'The Observatory'

An Old Idea

In a recent review[1], Heavens noted that "the notion of the de Sitter space-time as due to a fluid was not considered reasonable in 1973 since the pressure would be negative." Interestingly, that idea was first proposed by Erwin Schrödinger[2], just a few months after Einstein's first paper[3] on relativistic cosmology; Schrödinger noted "that the completely analogous system of solutions already exists for the field equations in their original form — without the terms [corresponding to the cosmological constant] introduced by Mr. Einstein [citation corresponding to my ref. 3]. The difference is superficially very small: The potentials remain unchanged, only the energy tensor of matter gets another form." [my translation]. Such a fluid has "a constant density and constant, spatially isotropic inner tension". I wonder if such a fluid would have been considered acceptable earlier if it was described as being under tension rather than having negative pressure.